Autonomously self-healing dielectric elastomer actuators from thermoplastic polydimethylsiloxane elastomer

Jeong, Seonghyeon; Skov, Anne Ladegaard; Daugaard, Anders E.

Published in:
Electroactive Polymer Actuators and Devices (EAPAD) XXIII

Link to article, DOI:
10.1117/12.2576864

Publication date:
2021

Document Version
Publisher's PDF, also known as Version of record

PROCEEDINGS OF SPIE

SPIEDigitalLibrary.org/conference-proceedings-of-spie

Autonomously self-healing dielectric elastomer actuators from thermoplastic polydimethylsiloxane elastomer

Jeong, Seonghyeon, Daugaard, Anders, Skov, Anne

Seonghyeon Jeong, Anders E. Daugaard, Anne L. Skov, "Autonomously self-healing dielectric elastomer actuators from thermoplastic polydimethylsiloxane elastomer," Proc. SPIE 11587, Electroactive Polymer Actuators and Devices (EAPAD) XXIII, 1158719 (15 December 2021); doi: 10.1117/12.2576864

SPIE.

Event: SPIE Smart Structures + Nondestructive Evaluation, 2021, Online Only

Autonomously self-healing dielectric elastomer actuators from thermoplastic polydimethylsiloxane elastomer

Seonghyeon Jeong[a,b], Anders E. Daugaard[a], Anne L. Skov[a]
[a] Danish Polymer Centre, Department of Chemical and Biochemical Engineering, Technical University of Denmark, Building 227, 2800 Kgs. Lyngby, Denmark; [b] Sino-Danish Center for Education and Research, University of Chinese Academy of Sciences, China

ABSTRACT

Dielectric elastomer actuators (DEAs) are usually operated at high voltage to induce sufficient electric pressure between two compliant electrodes sandwiching the dielectric elastomer. However, a harsh environment (e.g. humid environment combined with high voltage) often induces electrical breakdown (EB) of the DEAs, which results in pinhole formation or even tearing of the device, followed by macroscopic failure. Therefore, it is ideal for DEAs to be self-healing to extend robustness and lifetime, such as observed for biological muscles, which can be healed from injuries by inherent biological processes. Herein, we prepared a soft (Young's modulus: 187 kPa) polydimethylsiloxane (PDMS) thermoplastic elastomer (TPE) to demonstrate an autonomous self-healing ability. The system exploits hydrogen bonding (H-bonding) in two types of transient cross-linkers: urea group serves as a sacrificial bond under loading and ureidopyrimidone (UPy) serves as a strong, load-carrying crosslinker. The PDMS TPE shows a crossover of the elastic moduli at 119 °C and highly frequency dependent elastic modulus. The DEA is prepared with compliant, corrugated silver electrodes on both sides of a corrugated PDMS TPE film. A maximum actuation strain (6.8 % in longitudinal direction) is achieved at 18.8 V μm^{-1}. A further increase in potential does not increase the actuation strain, but EBs are observed on the electrodes and the actuation is maintained without any detrimental effects to the film despite the previous breakdown. The EBs do not form permanent pinholes, nor do they cause tearing of films. Instead, only the removal of the silver electrode is observed, which is the so-called self-clearing effect commonly observed for metallic electrodes. In combination with the self-clearing effect, the heat generated by the EBs allows the PDMS TPE to soften. The polymer molecules are then capable of flowing into the voids that were created at the initiation of the EBs. As a result, further propagation of the EB is hindered, and instead, an instantaneous and autonomous self-healing of the DEA is observed.

Keywords: PDMS, self-healing, DEA, thermoplastics, UPy

1. INTRODUCTION

DEAs consist of an elastomeric film with compliant electrodes on both sides of the elastomer.[1] When a voltage is applied to the electrodes, the generated electric pressure causes thinning of the elastomeric film between the electrodes. Consequently, the thinning of the elastomer induces lateral expansion of the DEAs because of the incompressibility of elastomers.[2] Due to this actuation behavior, the DEAs enable direct transformation of electrical energy to mechanical energy without the need of gearing. Therefore, the DEAs are often compared to biological muscles due to the similarity in the operation mechanism.[2,3]

Ideally, elastomers for DEAs should possess low Young's modulus, high dielectric permittivity, and sufficiently high electrical breakdown strength to achieve large actuation strains.[4] Albeit PDMS elastomers are widely used within soft robotics due to their inherent softness[5,6], they possess low dielectric permittivity.[7] Therefore, PDMS-based DEAs usually require high voltage to obtain large actuation strains, and this makes them prone to suffer from EB.[8]

The EB takes place via three stages.[9,10] The initiation of the electrical treeing arises rapidly during the inception stage from the defects within the elastomer. Then, the electrical tree propagates through the elastomer with a decelerated rate at the tree propagation stage. As the tip of the electrical tree approaches the electrode, the propagation rate of treeing is accelerated again and a pinhole is formed at the runaway stage. Simultaneously, the elastomer exhibits energy dissipation due to its viscoelasticity and current leakage.[11] In addition, the combination of Joule heating from the elastomer's resistance[12] and persistent plasma[13] after EB increases the temperature of the device and may result in either thermal or electrothermal breakdown of the DEA.

When the high voltage is maintained on the DEA after the EB, the pinhole serves as a short-circuit. Therefore, the DEA cannot create any electric pressure to induce the actuation after the EB but rather works as a conductor with the entire current going through the pinhole. This leads to increased pinhole size because of the dissipated energy.

Electroactive Polymer Actuators and Devices (EAPAD) XXIII, edited by Iain A. Anderson, Herbert R. Shea, John D. W. Madden, Proc. of SPIE Vol. 11587, 1158719
 · doi: 10.1117/12.2576864

Furthermore, due to PDMS-based elastomers' low tear strength, the EB usually leads to macroscopic tearing of the DEA, initiated from the pinhole.[14] Therefore, the EB usually terminates the function of DEAs.

From that perspective, the ideal DEA should be inherently self-healing during and after the EB to improve the reliability of the devices. However, current self-healing DEAs, e.g. silicone elastomers with silicone grease[15], may experience long-time stability issues from the migration of grease or delamination of electrodes. The usage of self-clearing electrodes[16], for which the EB locally burns the electrodes off to isolate the pinhole, may still cause detrimental failure to the DEA.[17] In addition, albeit the DEA manages to heal the pinhole from the EB, the required need of post-treatment, such as the application of temperature and pressure[10], is not ideal for use in commercial products.

In this work, we present an autonomously self-healing DEA after electromechanical breakdown. The self-healing behavior is achieved by utilizing the thermo-reversibility of the TPE in combination with self-clearing silver electrodes. The EB is observed as plasma, and the involved energies within the plasma induces the dissociation of the H-bonds of the PDMS TPE. As a result, the PDMS TPE flows and the voids created by the electrical treeing during the EB are healed and the electrical tree cannot propagate further.

2. EXPERIMENTAL

2.1 Preparation of PDMS TPE

The chain extension reaction is carried out between aminopropyl-terminated PDMS (10g, 0.477 mmoL) and hexamethylene diisocyanate (HMDI, 50 mg, 0.297 mmoL) in tetrahydrofuran (THF, 25 mL). After the reaction mixture is stirred for 7 hours at room temperature, the product is claimed by precipitation in methanol. The obtained product is further functionalized with the isocyanate-functionalized UPy (60 mg, 0.124 mmoL) in 300 mL THF by stirring the mixture for 48 hours. The final product is claimed from the THF by the precipitation in methanol, followed by drying for 3 days at 60 °C in vacuo, yielding a transparent elastic material. 17 wt% of silica (SIS6962.0) is added, turning the color of the elastomer to semi-transparent. The number-averaged molecular weight (Mn) of the polymer is determined to be 134,100 g mol^{-1} by size exclusion chromatography (SEC). (Yield: 85 %).

2.2 Fabrication of PDMS TPE-based DEA

The PDMS TPE is hot-pressed at 140 °C for 2 minutes within a 1 mm-thick square-shaped mold. Then, the elastomer is hot-pressed again at 120 °C in between two surface-corrugated release liners. The release liner's corrugation pattern is 10 μm distance between the pitches with 4 μm in depth. The surface-corrugated elastomer (average thickness: 160 μm) is cut into a rectangular shape (7 mm x 12 mm) where the corrugation is perpendicular to the longest dimension. The rim of the rectangle is covered by release liners. Then, the silver electrodes are sputter-coated onto both sides of the elastomeric film within a specific area (5 mm x 10 mm).

2.3 Mechanical characterization

The specimens for tensile tests, successive cyclic tensile tests, and successive stress relaxation tests are prepared according to ASTM D638 type V. The gauge length (L_0) is set to be 33 mm with the elongation rate of 30 mm min^{-1} unless specified otherwise. Strain is defined as $(L - L_0)/L_0$ where L is the distance between the two grips during the uniaxial elongation. Engineering stress is calculated from the measured stress divided by the initial cross-sectional area of the specimens. The Young's modulus is determined by linear fitting of the initial slope (up to approximately 10 % strain) of the stress-strain curve. The cyclic tensile tests are carried out by applying a strain of 300 % 5 times, and the 6th cycle is carried out after the sample is allowed to cool to room temperature without external stress for 1 hour. 10 adjacent data points are averaged to eliminate noise for both types of mechanical tests. Hysteresis is calculated as the difference between areas under the loading and unloading curves, respectively. The successive stress relaxation tests are conducted 3 times for 300 seconds with a pre-set 10 % of strain. The following cycles are carried out immediately after the grips are recovered to their original positions.

2.4 Actuation test

The DEA is vertically attached onto a stand such that the corrugation lines horizontally aligned. Both top and bottom ends of the DEA are covered with polyimide-based tape to inhibit a detouring of the current. On the bottom side of the DEA, a mass of 1045 mg is added. A step-wise increasing electric field is applied by a high voltage power supply (PS375, Stanford Research Systems) through two copper wires attached to each of the dielectric elastomer's electrodes. To avoid the direct contact of the copper wires to the silver electrodes, carbon grease is used between the electrodes and the copper wires.

2.5 Rheological characterization

Rheological properties of the PDMS TPE are measured by a rheometer (Discovery HR-1, TA) equipped with parallel-plate geometry (diameter: 12 mm). Temperature sweep test is conducted at a fixed strain amplitude (1 % strain, 40 rad s^{-1}) from 200 °C to 25 °C, at a cooling rate of 5 °C min^{-1}. Frequency sweep tests are performed with the same amplitude from a frequency range from 300 rad s^{-1} to 10^{-1} rad s^{-1} at different temperatures (25 - 170 °C). Oscillatory time sweep tests at two temperatures of 25 °C and 140 °C, respectively, are conducted to simulate melting and solidifying of the PDMS TPE. For each cycle, the temperature is kept constant at the given temperature for 10 minutes and then followed by cooling/ heating and equilibrating for 3 minutes.

3. RESULTS AND DISCUSSION

3.1 The design of PDMS TPE

In this work, the chain extension reaction is carried out between HMDI and long PDMS chains (Mn: 21,000 g mol^{-1}, determined by ^{1}H-NMR). Then, the chain ends are end-capped by urea-adjacent UPys, to yield a soft PDMS TPE (Figure 1a). The chain extension reaction yields amine-terminated linear PDMS chains with urea groups, showing no elastic behavior but rather plastic-like deformation (Mn: 170,900 g mol^{-1}, determined by SEC). It indicates the weakly associated dynamic H-bonds of urea groups.[18] However, when the chain ends are end-capped by urea-adjacent UPy, a soft elastomer is yielded due to the strong physical interaction. This strong interaction between the urea-adjacent UPys results from the dimerization of the UPys via a unique self-complementary association of quadruple H-bonds.[19,20] In addition, the dimers show a laterally stacked structure due to the UPy being adjacent to additional H-bonds.[21,22] Therefore, the urea-adjacent UPys can serve as strong physical cross-linkers, while the urea groups between the PDMS chains serve as weak H-bonds due to the high mobility (Figure 1b).

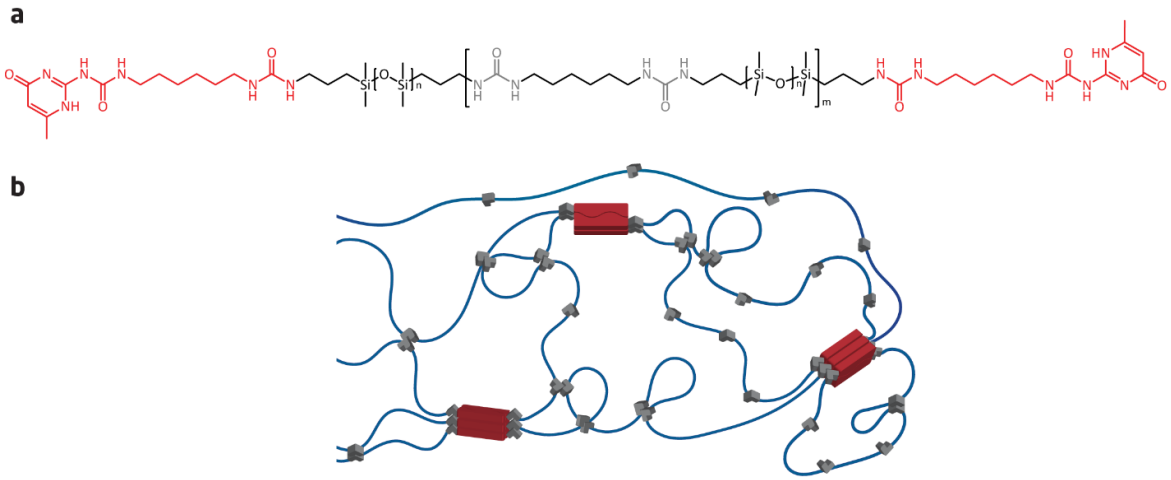

Figure 1. (a) Chemical structure of the PDMS TPE. The PDMS chains are physically linked to each other via the urea groups (grey), and the urea-linked PDMS chains are end-capped by urea-adjacent UPys (red). (b) Schematic illustration of the PDMS TPE structure. The laterally stacked structure of UPy dimers (red) and the sacrificial H-bonds from urea groups (grey) are shown.

The PDMS TPE exhibits elongation rate-dependent mechanical properties in tensile tests (Figure 2a). The slower elongation rates show a lower Young's modulus accompanied by a lower stress at break, indicating a dynamic exchange of H-bonds during the elongation. At the lowest elongation rate of 30 mm min^{-1}, the Young's modulus is determined to 187 kPa. The tensile stress shows a plateau above 380 % strain, which is not observed at faster elongation rates. This plateau in engineering stress indicates a linear relationship between stress and strain with a modulus equal to the inverse strain. We hypothesize that this low elastic modulus before the failure of the specimen results from the sliding of the laterally stacked UPy structure.

The relaxation time (τ) of the dynamic strands in network is proportional to the inverse crossover frequency ($\tau = 1/(2\pi f)$), where f is frequency in Hz. Therefore, τ is calculated from the master curve of storage modulus (G') and loss modulus (G") at 25 °C (Figure 2b). Any deformation conducted on a slower time-scale than τ results in a viscous response of the network rather than an elastic response. The viscous contribution arises from the sliding of the laterally stacked UPy structure of the PDMS TPE. The time-scales for the elongations are determined from the Hencky strain rate ($\dot{\varepsilon}_H = (dL/dt)/L(t)$) , where dL/dt is the change in length with time.[23] The inverse Hencky strain rates ($1/\dot{\varepsilon}_H$) are plotted against the strain at different elongation rates (Figure 2c) to give an idea of the permissible time-scales for relaxation at different stages of the elongations. Subsequently, the time-scalesf are compared to τ of the

network. The comparisons show that the time-scales ($1/\dot{\varepsilon}_H$) of the three largest elongation rates are always faster than the relaxation time (τ =159 s) of the network until the failures of the specimens. On the other hand, the time-scale of the lowest elongation rate decreases along the elongation and then exceed the τ of the network at a certain stage of the elongation. Therefore, the PDMS TPE shows the above-mentioned low elastic modulus along the elongation.

The successive cyclic tensile tests to 300 % elongation show that the PDMS TPE is able to maintain the internal stress for 300 % strain during the deformation cycles owing to the above-mentioned intact structure of the UPys (Figure 2d). On the other hand, the rapidly decreased Young's modulus and hysteresis along the cycles indicate dissociation of H-bonded urea groups along the repeated elongations. When the elastomer is relaxed at room temperature for an hour after the 5th cycle, the moderate recovery of both Young's modulus and hysteresis at 6th cycle suggests re-formation of the H-bonds of the urea groups, while the rearrangement of the H-bonds is responsible for the softening behavior of the elastomer.

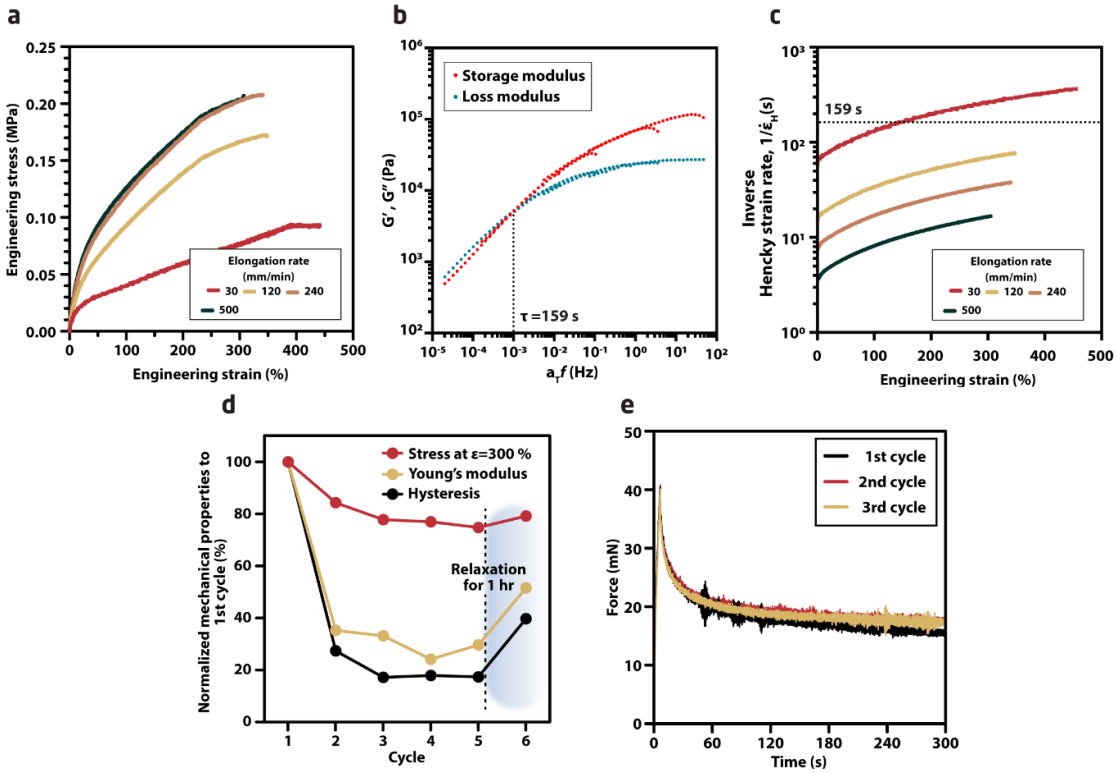

Figure 2. (a) Tensile tests of the elastomer for different elongation rates. (b) Master curve of storage modulus (G') and loss modulus (G") at T_{ref} = 25 °C. The crossover frequency is marked (dashed line), and the relaxation time is calculated from the crossover frequency. (c) Calculated inverse Hencky strain rates at different elongation rates. The relaxation time (τ = 159 s) of the network strands in linear flow is marked (dashed line). (d) The change in mechanical properties along successive cyclic tensile tests. The data of the following cycles (2nd-6th cycles) are normalized to the ones from the 1st cycle. (e) Successive stress relaxation tests where the specimen is exposed to 10 % strain for 300 seconds for each cycle. The grips are recovered to their original position after 300 s, and the subsequent cycles are carried out immediately without giving the specimen time to relax between the cycles.

During the stress relaxation tests, the specimen stays at 10 % strain for 300 s for each cycle. As the grips recover their original positions at the end of the cycle, the subsequent stress relaxation tests are repeated twice under identical conditions. When elastomers are elongated, entropy drives the recovery of classical covalently bonded elastomers to their original zero stress states. On the other hand, TPEs may dissipate the imposed mechanical energy through plastic deformation, resulting in a permanent set. As a result, a full recovery is challenging for TPEs. However, the results from the successive stress relaxation tests show identical maximum force and stress relaxation profile, indicating a fully recovered PDMS TPE after each cycle (Figure 2e). It suggests that the H-bonded structures are intact under small strains (as also observed from the successive cyclic tensile tests). Therefore, the PDMS TPE can avoid significant viscous losses for small deformation and thereby resemble classical elastomers.

3.2 Instantaneous self-healing DEA from electrical breakdowns

The DEA is prepared from the PDMS TPE and the compliant electrodes with corrugations on both sides of the elastomer. The actuation strain is calculated from the ratio of length change to the original length of the DEA (Figure 3a). The DEA shows larger actuation strain with increase in the given voltage, as expected from the actuation equation.[24] However, this trend is only followed up to 18.8 V μm^{-1} where the DEA shows 6.8 % of actuation strain. A further increase in voltage does not result in larger actuation strain (< 4.1 % actuation strain). Instead, the DEA shows a continuous breakdown (Figure 3b).

The EBs remain on the surface of the electrodes, and they appear as persistent plasma, while the DEA shows no leakage current. It suggests that there is no macroscopic failure, such as pinhole formation and tearing. Instead, the DEA only shows a color change on the electrodes (Figure 3c). The surface areas, where the EBs appear, are illustrated in red color (Figure 3d) and are examined with an optical microscope (Figure 3e).

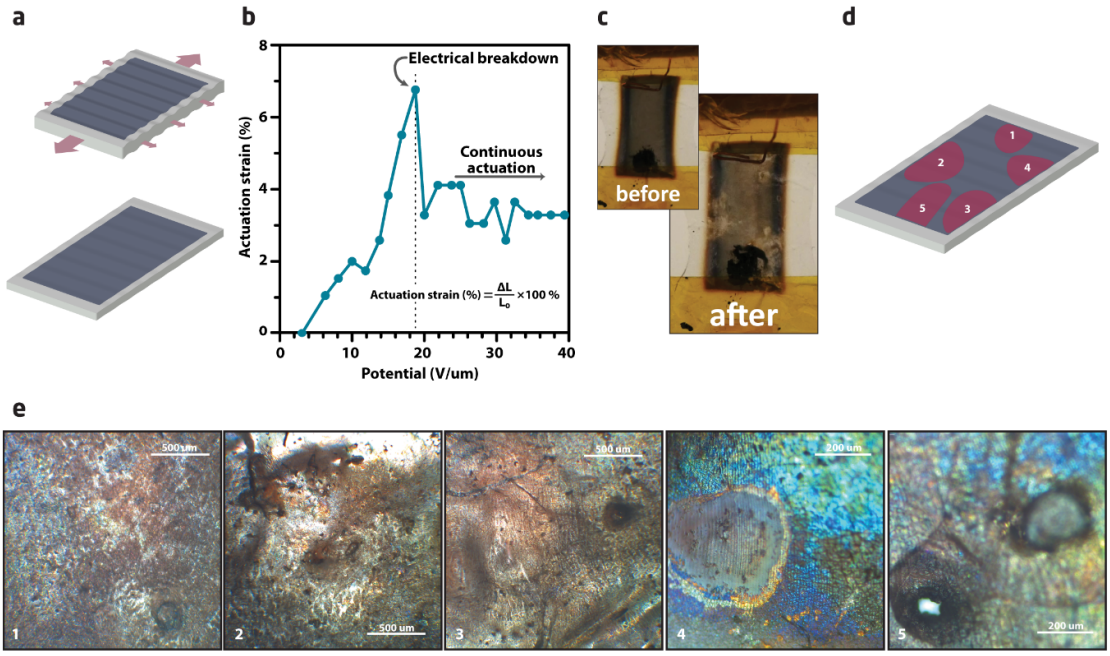

Figure 3. (a) Illustration of bilateral actuation of the surface-corrugated DEA. (b) Obtained actuation strain along the increase in the given potential. (c) The visible color change of the electrode before and after the EBs. (d) Schematic illustration of simplified electrode areas where the color change is observed. (e) Microscopic images obtained from the electrode surface. The numbers on each image indicate where on the electrode (illustrated in d) the image is obtained.

The DEA shows no pinholes and yet the self-clearing effect of the electrodes can be observed (1-3, Figure 3e). The self-clearing effect assists the termination of the EB process since there is no voltage at the electrode-free area. This effect is clearly observed as a pinhole-like trace in the middle of the electrode-free area (4, Figure 3e). For the investigated films, the EBs do not give rise to macroscopic failure unless the voltage is continuously increased after the initial breakdown. The pinhole formation by the EB is observed at 45.6 V μm^{-1}, which is 2.4 times higher than the voltage where the initial EB is observed (5, Figure 3e).

The DEA survives from the repeated EBs, owing to the instantaneous and autonomous self-healing capability. This capability is achieved since the self-healing rate of the DEA is faster than the propagation of the electrical treeing during the EBs.[9]

3.3 The origin of instantaneous self-healing from electrical breakdowns

When the electrical treeing creates the cracks or the voids within the DEA, the combination of persistent plasma and the dissipative losses of the DEA increases the temperature of the DEA. In this regard, the fully dissociated H-bonds of the PDMS TPE at 119 °C can be seen from the temperature sweep test from the crossover between G' and G" (Figure 4a). The flow of the PDMS TPE dissipates heat energy through the rearrangement of the dissociated H-bonds at the raised temperature. Consequently, the rearrangement of H-bonds around the cracks and voids enables the self-healing of the DEA.

The above-mentioned rearrangement of H-bonds must be rapid to govern the instantaneous self-healing during the EB. A measure for the rearrangement of the H-bonds can be provided from the relaxation time (τ), which can be considered as the averaged bond lifetime ($\bar{\tau}_b$) at a given temperature.[18,25] In this regard, $\bar{\tau}_b$ is directly calculated from the frequency sweep tests at different temperatures (Figure 4b). The increased temperature from 25 °C to 110 °C, 140 °C, and 170 °C results in a decrease in $\bar{\tau}_b$ from 159 s to 0.38 s, 0.03 s, and less than 0.01 s at the respective temperatures. The shorter $\bar{\tau}_b$ of the H-bonds at higher temperatures indicates a more dynamic rearrangement, as expected.

A previous study showed urea groups-based supramolecular PDMS TPEs which possess glass transition temperatures of -9 °C to - 21 °C and which are autonomously self-healing under ambient conditions when their $\bar{\tau}_b$ are less than 100 s at room temperature.[18] In particular, when $\bar{\tau}_b$ are less than 10 s, the self-healing efficiencies (ratio of strain or stress of healed samples to the original values) approached more than 70 % in a strain recovery mode and more than 90 % in their respective stresses after 12 hours of the healing process at room temperature.

In the same manner, the PDMS TPE was shown exhibits rapid self-healing behavior with the shortened $\bar{\tau}_b$ at raised temperatures.

In addition, the shortened $\bar{\tau}_b$ enables a dynamic stress response at the two given temperatures (25 °C and 140 °C), where the PDMS TPE can recover its original mechanical properties at 25 °C (Figure 4c). It suggests that the self-healing behavior at a raised temperature (as observed from the frequency sweep tests) does not change the mechanical properties of the PDMS TPE after the healing process.

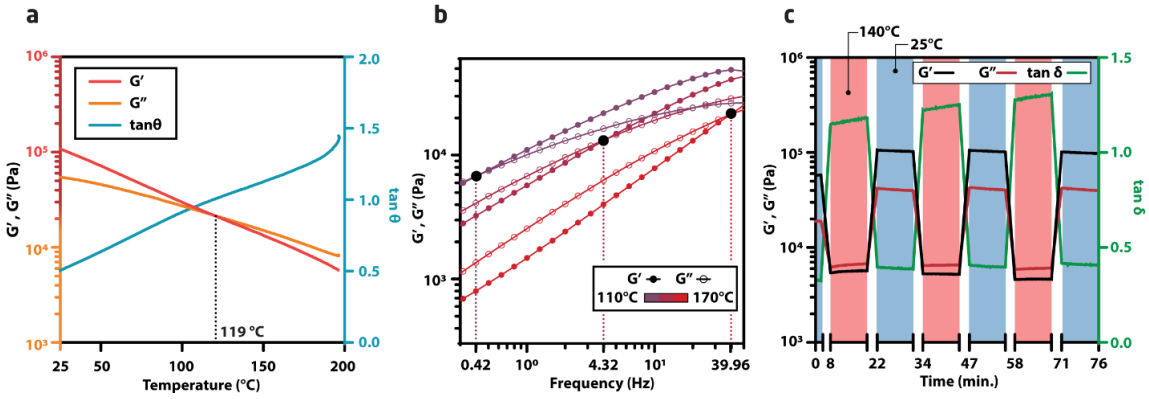

Figure 4. Rheological properties. (a) Temperature sweep test. (b) Frequency sweep tests at three different temperatures. The black circles indicate the frequencies where storage modulus (G') and loss modulus (G") cross over. (c) Oscillatory time sweep tests. The moduli are continuously measured at alternate 25 °C (blue) and 140 °C (red).

4. CONCLUSION

We developed a soft PDMS TPE by the combination of urea and urea-adjacent UPy with PDMS, exploiting the dynamic association of H-bonds with the intact UPy structure under deformation. The PDMS TPE shows a temperature and frequency dependent elastic modulus, and the temperature strongly affects the bond lifetime of the reversible network. A self-healing DEA was fabricated by utilizing the shortened bond lifetime of the PDMS TPE at a raised temperature. Owing to the instantaneous and autonomous self-healing capability of the DEA, the electromechanical breakdown does not yield macroscopic failure of the DEA, while it can be easily observed as plasma on the electrodes. Therefore, this DEA can be operated within the optimal voltage to maximize the actuation, while avoiding the further electrical breakdown or macroscopic failure. This novel approach to fabricate a self-healing DEA provides a new route to solve intricate problems of the current DEAs.

5. REFERENCES

[1] Madsen, F. B., Daugaard, A. E., Hvilsted, S. & Skov, A. L. The Current State of Silicone-Based Dielectric Elastomer Transducers. *Macromolecular Rapid Communications* **37**, 378–413 (2016).

[2] Brochu, P. & Pei, Q. Advances in Dielectric Elastomers for Actuators and Artificial Muscles. *Macromolecular Rapid Communications* **31**, 10–36 (2010).

[3] Duduta, M., Hajiesmaili, E., Zhao, H., Wood, R. J. & Clarke, D. R. Realizing the potential of dielectric elastomer artificial muscles. *Proceedings of the National Academy of Sciences* **116**, 2476–2481 (2019).

[4] Skov, A. L. & Yu, L. Optimization Techniques for Improving the Performance of Silicone-Based Dielectric

Elastomers. *Advanced Engineering Materials* **20**, 1–21 (2018).

[5] Hines, L., Petersen, K., Lum, G. Z. & Sitti, M. Soft Actuators for Small-Scale Robotics. *Advanced Materials* **29**, 1603483 (2017).

[6] Hu, P., Madsen, J., Huang, Q. & Skov, A. L. Elastomers without covalent cross-linking: Concatenated rings giving rise to elasticity. *ACS Macro Letters* **9**, 1458–1463 (2020).

[7] Yu, L., Madsen, F. B. & Skov, A. L. Degradation patterns of silicone-based dielectric elastomers in electrical fields. *International Journal of Smart and Nano Materials* **9**, 217–232 (2018).

[8] Madsen, F. B., Yu, L., Daugaard, A. E., Hvilsted, S. & Skov, A. L. Silicone elastomers with high dielectric permittivity and high dielectric breakdown strength based on dipolar copolymers. *Polymer* **55**, 6212–6219 (2014).

[9] Yang, Y., Dang, Z. M., Li, Q. & He, J. Self-Healing of Electrical Damage in Polymers. *Advanced Science* **2002131**, 1–21 (2020).

[10] Zhang, Y. *et al.* Electrical and Mechanical Self-Healing in High-Performance Dielectric Elastomer Actuator Materials. *Advanced Functional Materials* **29**, 1808431 (2019).

[11] Chiang Foo, C., Cai, S., Jin Adrian Koh, S., Bauer, S. & Suo, Z. Model of dissipative dielectric elastomers. *Journal of Applied Physics* **111**, 034102 (2012).

[12] Christensen, L. R., Hassager, O. & Skov, A. L. Electro-Thermal model of thermal breakdown in multilayered dielectric elastomers. *AIChE Journal* **65**, 859–864 (2018).

[13] La, T.-G. & Lau, G.-K. Inhibiting electro-thermal breakdown of acrylic dielectric elastomer actuators by dielectric gel coating. *Applied Physics Letters* **108**, 012903 (2016).

[14] Zakaria, S., Morshuis, P. H. F., Benslimane, M. Y., Yu, L. & Skov, A. L. The electrical breakdown strength of pre-stretched elastomers, with and without sample volume conservation. *Smart Materials and Structures* **24**, 055009 (2015).

[15] Hunt, S., McKay, T. G. & Anderson, I. A. A self-healing dielectric elastomer actuator. *Applied Physics Letters* **104**, 1–4 (2014).

[16] Yuan, W. *et al.* Fault-Tolerant Dielectric Elastomer Actuators using Single-Walled Carbon Nanotube Electrodes. *Advanced Materials* **20**, 621–625 (2008).

[17] Rosset, S. & Shea, H. R. Flexible and stretchable electrodes for dielectric elastomer actuators. *Applied Physics A: Materials Science and Processing* **110**, 281–307 (2013).

[18] Döhler, D. *et al.* Tuning the Self-Healing Response of Poly(dimethylsiloxane)-Based Elastomers. *ACS Applied Polymer Materials* **2**, 4127–4139 (2020).

[19] Meng, Y., Xu, W., Newman, M. R., Benoit, D. S. W. & Anthamatten, M. Thermoreversible Siloxane Networks: Soft Biomaterials with Widely Tunable Viscoelasticity. *Advanced Functional Materials* **1903721**, 1903721 (2019).

[20] Sijbesma, R. P. *et al.* Reversible Polymers Formed from Self-Complementary Monomers Using Quadruple Hydrogen Bonding. *Science* **278**, 1601–1604 (1997).

[21] Botterhuis, N. E., van Beek, D. J. M., van Gemert, G. M. L., Bosman, A. W. & Sijbesma, R. P. Self-assembly and morphology of polydimethylsiloxane supramolecular thermoplastic elastomers. *Journal of Polymer Science Part A: Polymer Chemistry* **46**, 3877–3885 (2008).

[22] Liu, M., Liu, P., Lu, G., Xu, Z. & Yao, X. Multiphase-Assembly of Siloxane Oligomers with Improved Mechanical Strength and Water-Enhanced Healing. *Angewandte Chemie International Edition* **57**, 11242–11246 (2018).

[23] Tran, J.-A., Madsen, J. & Skov, A. L. Novel polyrotaxane cross-linkers as a versatile platform for slide-ring silicone. *Bioinspiration & Biomimetics* (2021) in press doi:10.1088/1748-3190/abdd9f.

[24] Pelrine, R., Kornbluh, R. & Kofod, G. High-Strain Actuator Materials Based on Dielectric Elastomers. *Advanced Materials* **12**, 1223–1225 (2000).

[25] Bose, R. K., Hohlbein, N., Garcia, S. J., Schmidt, A. M. & van der Zwaag, S. Connecting supramolecular bond lifetime and network mobility for scratch healing in poly(butyl acrylate) ionomers containing sodium, zinc and cobalt. *Physical Chemistry Chemical Physics* **17**, 1697–1704 (2015).